^{7}Li($\vec{p},\pi^-$)^{8}B* and ^{7}Li($\vec{p},\pi^+$)^{8}Li* reactions in the region of the Δ_{1232} resonance

G. M. Huber* and G. J. Lolos
Department of Physics and Astronomy, University of Regina, Regina, Canada S4S 042

K. M. Furutani and W. R. Falk
Department of Physics, University of Manitoba, Winnipeg, Canada R3T 2N2

R. D. Bent
Indiana University Cyclotron Facility, Bloomington, Indiana 47408

K. H. Hicks,† P. L. Walden, and S. Yen
TRIUMF, Vancouver, British Columbia, Canada V6T 2A3

(Received 29 April 1988)

Differential cross sections and analyzing powers for the ^{7}Li($\vec{p},\pi^\pm$) reactions leading to discrete states of ^{8}B and ^{8}Li, as well as to the continuum, are presented at $T_p=280$, 354, and 489 MeV. These results are compared with previously published results at 200 and 250 MeV. At fixed four-momentum transfers squared in the region $0.6>t>0.4$ GeV$^2/c^2$, the energy dependence of the (p,π^+) and (p,π^-) differential cross sections is quite similar, in sharp contrast to earlier results from the ^{13}C$(p,\pi^\pm)$ reactions. The observed variations in the (p,π^-) energy dependence are presumed to reflect differences in the relative importance of resonant and nonresonant amplitudes in the (p,π^-) reaction mechanism. The analyzing powers of the $(\vec{p},\pi^-)$ and $(\vec{p},\pi^+)$ reactions are qualitatively very similar except for a difference in sign.

I. INTRODUCTION

Over the past few years there has been sustained interest in (p,π) reactions. A number of reviews[1–4] summarize the work in this field up to about the time of the Indiana Pion Production and Absorption Workshop.[5] Since then, there have been a number of notable developments, of which the discovery[6] of the previously unsuspected selectivity of (p,π^-) reactions for the population of high-spin two-particle–one-hole ($2p$-$1h$) states has perhaps generated the most interest. The discovery was part of a larger program of the study of (p,π^-) reactions at the Indiana University Cyclotron Facility (IUCF) which demonstrated the two-nucleon nature of the (p,π^-) reaction mechanism. A recent publication by Throwe *et al.*[7] summarizes work done on calcium isotopes and includes references to earlier work.

A recent parallel development has been the systematic study at TRIUMF of the energy dependence of (p,π) reactions in the region of the Δ_{1232} resonance.[8–12] This study has shown that (p,π^+) reactions generally have an energy dependence similar to that of the $pp\rightarrow d\pi^+$ reaction after transformation to the nuclear kinematical frame. This has been interpreted as strong evidence of a significant role of $NN\rightarrow N\Delta\rightarrow NN\pi^+$ processes in the (p,π^+) reaction mechanism.

Little is known about the energy dependence of the (p,π^-) reaction in the Δ_{1232} region. A preliminary investigation at TRIUMF[13] showed that the ^{18}O$(p,\pi^-)^{19}$Ne$^*_{4.6}$ reaction had an energy dependence similar to that of the ^{12}C$(p,\pi^+)^{13}$C$^*_{9.5}$ reaction, and this was interpreted to indicate that the influence of the Δ_{1232} resonance was seen in both reactions, although perhaps more weakly in the (p,π^-) reaction than in the (p,π^+) reaction. In a more recent study,[11] a striking difference was observed between the energy dependences of the (p,π^+) and (p,π^-) reactions on ^{13}C leading to mirror final states, suggesting that the role of the Δ_{1232} is distinctly different in these two reactions. By comparing transitions to mirror final states, effects due to differences in nuclear structure are minimized, so that the differences in the energy behavior of the (p,π^+) and (p,π^-) differential cross sections at the same four momentum transfer squared should reflect primarily differences in reaction mechanism rather than nuclear structure. The (p,π^+) reactions exhibited the very familiar strong enhancement of the differential cross section near the Δ_{1232} invariant mass, whereas the (p,π^-) reactions showed no enhancement of the differential cross section in the region of the Δ_{1232} invariant mass. These differences were observed for transitions to the ground states of the mirror nuclei, as well as to mirror excited states whose nuclear structure is substantially different from the ground state. Thus there appears to be a substantial difference in the role of the Δ_{1232} in these particular (p,π^+) and (p,π^-) transitions.

Differences between the (p,π^+) and (p,π^-) reactions are not unexpected since the two reactions go through different spin and isospin channels. In a two-nucleon mechanism, the dominant amplitude for the elementary $pp\rightarrow pn\pi^+$ process, via an intermediate Δ-N system, is forbidden for the $pn\rightarrow pp\pi^-$ process by angular momentum and parity conservation and the Pauli exclusion prin-

ciple. Other weaker resonant amplitudes may contribute to the (p,π^-) reaction, but can be masked by nonresonant amplitudes of comparable magnitude.

It is important to have information on the energy dependence of the (p,π^-) reaction for other targets in order to determine whether the apparent suppression of the Δ_{1232} contribution in the ^{13}C$(p,\pi^-)^{14}$O* reaction is peculiar to the particular transitions studied, or is a general feature of the (p,π^-) reaction. Furthermore, the ^{13}C$(p,\pi^\pm)$ comparisons of Ref. 11 were made at only one value of the four momentum transfer squared, $t=0.50$ GeV$^2/c^2$, which is nearly the smallest t value accessed at 180 MeV and nearly the largest value of t accessed at 489 MeV.

The results reported here were obtained in order to shed light on the role of the Δ_{1232} resonance in the (p,π^+) and (p,π^-) reactions. ^{7}Li was chosen as the target nucleus for these investigations because, as for ^{13}C$(p,\pi^\pm)$, the ^{7}Li$(p,\pi^-)^8$B and ^{7}Li$(p,\pi^+)^8$Li reactions lead to mirror final states, thus minimizing nuclear structure differences between the two reactions. In addition, the low-lying states of ^{8}B and ^{8}Li are widely spaced and easily resolvable with the medium resolution spectrometer (MRS) spectrometer at TRIUMF. These advantages, together with the higher yields resulting from thicker targets, allowed the energy dependence of the (p,π^-) reaction to be studied for the first time over a range of t values. These results can be combined with those obtained at IUCF at 200 MeV (Ref. 14) and at TRIUMF at 250 MeV (Ref. 9) to provide information over a wide energy range.

II. THE EXPERIMENT

A number of papers[8–12] on (p,π) experiments performed at TRIUMF have been published recently. For detailed information on the experimental techniques and data analysis methods employed in these experiments, the reader is referred to Ref. 15. A brief description of these procedures and differences between the present and earlier experiments follows.

This experiment was performed with the MRS at TRIUMF.[16] This spectrometer, shown in Fig. 1, is a 1.4 GeV/c quadrupole-dipole system that is located on beam line BL4B in the TRIUMF proton hall. The spectrometer detection system consists of a horizontal drift chamber located in front of the spectrometer's entrance quadrupole magnet [the front end chamber (FEC)], and two vertical drift chambers (VDC) followed by two planes of plastic scintillators located near the focal plane of the spectrometer. A twister, consisting of six quadrupole magnets, allows, in principle, for the use of a dispersion matched beam in order to take advantage of the good resolution obtainable with the MRS. Perfect dispersion matching requires the use of a -23 cm/% beam tune for (p,π) data taking at 354 MeV, and an even larger beam dispersion at 280 MeV. However, the large momentum spread of the proton beam, and the limited beam size that can be reliably handled in the beam line, allowed a dispersion of only -12 cm/% to be used.

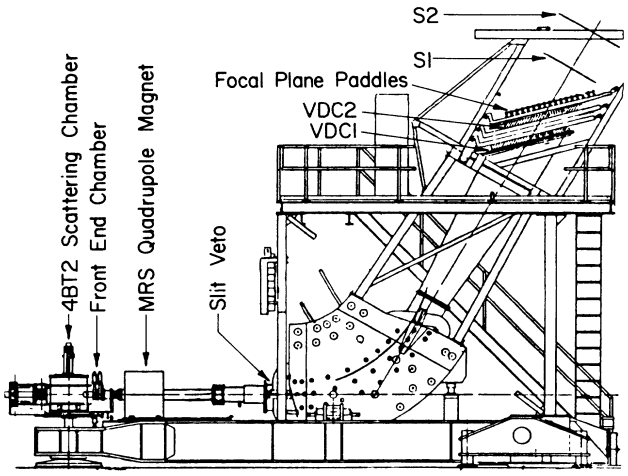

FIG. 1. The medium resolution spectrometer.

Thus the resolution obtained in this experiment was not as good as what one is normally able to attain with the MRS, but was adequate to resolve the final states of interest in ^{8}Li and ^{8}B.

The experiment used polarized proton beam intensities between 2 and 55 nA, with an intensity less than 15 nA used for most runs except those at extreme back angles. The maximum beam intensity was chosen to keep the counting rate on the entire FEC below 1 MHz. Beam polarization was typically 68% at 280 MeV, 66% at 354 MeV, and 45% at 489 MeV. The beam was incident on metallic ^{7}Li targets of 211 ± 1.5 mg/cm^2 and 450.5 ± 0.6 mg/cm^2 thickness for the (p,π^+) and (p,π^-) runs, respectively. The thicker target degraded the energy resolution, but was necessary to make the (p,π^-) measurements feasible within the allotted beam time.

The spectrometer acceptance was calibrated using the $pp\rightarrow d\pi^+$ reaction[17] at the beginning and at the end of the experiment at 489 MeV and $\theta_{\rm lab}=24.6°$, and at 354 MeV and $\theta_{\rm lab}=31.7°$ in the middle of the experiment. Pions from this reaction at 489 MeV have approximately the same momentum as pions from the ^{7}Li(p,π) reaction at 354 MeV, and pions from the $pp\rightarrow d\pi^+$ reaction at 354 MeV have approximately the same momentum as pions from the ^{7}Li(p,π) reaction at 280 MeV. The effective solid angle of the spectrometer, determined by this method, was 2.82 ± 0.1 msr at 489 MeV and 2.62 msr at 354 MeV. Thus 2.82 msr was used for the spectrometer solid angle for the 354 and 489 MeV ^{7}Li(p,π) data, and 2.62 msr was used for the spectrometer solid angle for the 280 MeV data. The uncertainty in the lower energy solid angle calibration was taken to be the same as that in the higher energy calibration.

Finally, all data were corrected for event losses in the nonbend plane of the spectrometer due to improper setting of the spectrometer quadrupole field, which caused the image size to be larger than the aperture of the VDC in the nonbend plane. A sample histogram showing this

effect is given in Fig. 2. This correction was accomplished by assuming that the histogram shown in Fig. 2 should be symmetric about the position of the central ray. The value of this correction varied from run to run, but was approximately 37% for the 280 and 354 MeV runs and 3% for the 489 MeV runs. The accuracy of this correction was tested by comparing the two sets of $pp \rightarrow d\pi^+$ calibrations at 489 MeV in which this factor was approximately 28% in the first scan, and approximately 10% in the second scan. It was found that the effective solid angles for the two scans were the same to within 1% after correcting for this loss.

The systematic uncertainty in the cross sections measured in this experiment is ±7% and is dominated by the uncertainty in the solid angle (±6%). The relative uncertainty is ±12% and is dominated by the sensitivity of the results to the placement of software cuts in the data analysis (±8%), and by the uncertainty in the nonbend plane correction factor (±7%). The sensitivity of the results to errors in the data analysis was estimated by analyzing some data twice, with different solid angle, beam spot, and particle trajectory cuts.

III. RESULTS

Figures 3 and 4 show sample pion spectra taken at proton bombarding energies of 280, 354, and 489 MeV and scattering angles corresponding to the same value of the square of the four momentum transfer ($t = 0.40$ GeV$^2/c^2$) at each energy. Thus Figs. 3 and 4 depict the rough energy dependence of the ^{7}Li$(p,\pi^-)^8$B* and ^{7}Li$(p,\pi^+)^8$Li* reactions. The most striking difference between the two figures is that the continuum becomes progressively more dominant in the (p,π^-) spectra relative to the discrete states as the proton energy increases, whereas the discrete states dominate the (p,π^+) spectra at all energies. A similar suppression of (p,π^-) transitions to discrete states was observed in a comparison of the ^{13}C$(p,\pi^\pm)$ reactions.[12]

Differential cross sections and analyzing powers for the (p,π^+) and (p,π^-) reactions leading to the three low-

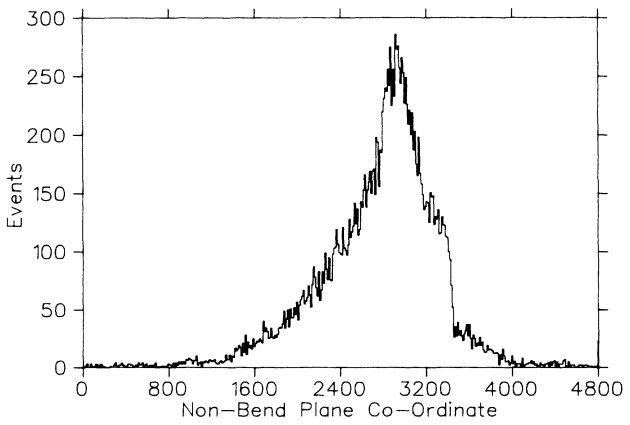

FIG. 2. Histogram of the nonbend plane coordinate of the VDC closest to the focal plane from the first $pp \rightarrow d\pi^+$ scan showing the effect of improper setting of the MRS quadrupole field. The correction factor for this run was 25%.

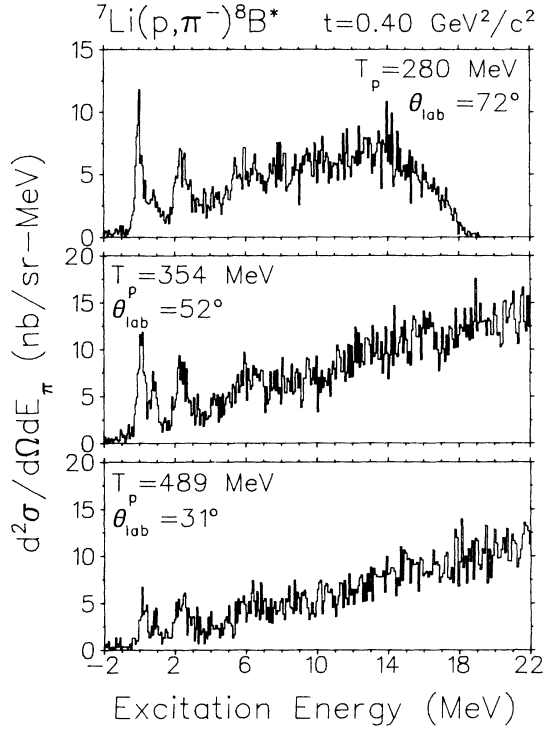

FIG. 3. Pion spectra of the ^{7}Li$(p,\pi^-)^8$B* reaction. The 280 MeV momentum acceptance of the MRS only allowed data to be taken up to an excitation energy of approximately 15 MeV; the drop in cross section above this excitation is instrumental in nature. At the higher energies, the momentum acceptance of the MRS allowed data from a much larger range of excitation energies to be taken.

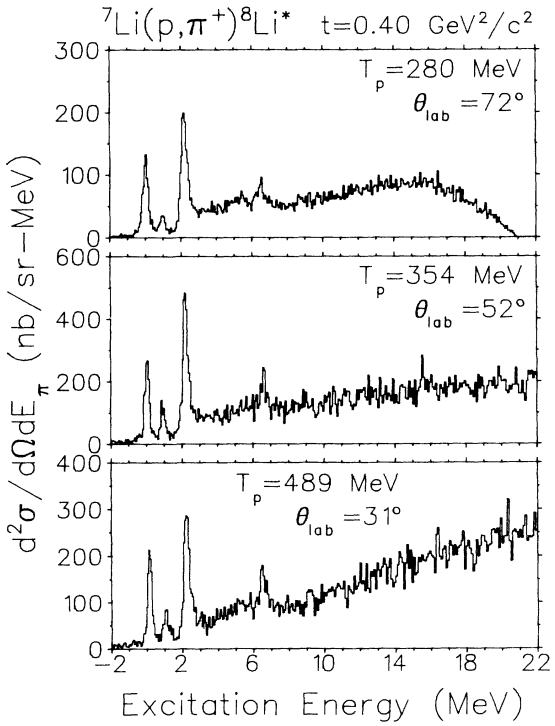

FIG. 4. Pion spectra of the ^{7}Li$(p,\pi^+)^8$Li* reaction. The experimental resolution for these spectra, approximately 330 keV, is better than in the spectra of Fig. 3 because a thinner ^{7}Li target was used.

lying states of ^8Li and ^8B are listed in Tables I and II. The data listed in Table II are the first (p,π^-) data taken in the Δ_{1232} region that spans a range of t values.

IV. ENERGY DEPENDENCE OF THE DIFFERENTIAL CROSS SECTIONS

Figures 5–10 show the energy dependence of the $^7Li(p,\pi^-)^8B$ and $^7Li(p,\pi^+)^8Li$ reactions leading to the three lowest-lying states of the final nuclei. Figures 5–7 show that, except for the 200 MeV data at small t values, the $^7Li(p,\pi^-)^8B^*$ differential cross sections peak in the neighborhood of the Δ_{1232} resonance ($T_p=343$ MeV, or $\sqrt{s}-m_A=1.232$ GeV). At small values of t, the 200 MeV $^8B^*_{2.32}$ differential cross sections are larger than those at higher energies. The differential cross section enhancement at large angles (small t) is a common feature of (p,π) reactions at low energies and appears to be nuclear structure related.[18]

The $^7Li(p,\pi^+)^8Li$ data shown in Figs. 8–10 exhibit a similar energy dependence. This type of energy dependence has been previously observed in other (p,π^+) reactions,[8] except that the decrease in cross section above the Δ_{1232} resonance is less for the $^7Li(p,\pi^+)^8Li$ reaction than in most other cases. The agreement between the old[9] and present data sets at 354 MeV near $t=0.4$ GeV$^2/c^2$ is well within statistic errors for the $^8Li^*_{2.255}$ state, but there is a 25% discrepancy between the two data sets for the $^8Li_{g.s.}$ and $^8Li^*_{0.9808}$ states. The older data were obtained from the high excitation end of the MRS focal plane in an $^{16}O(p,\pi^+)^{17}O$ experiment using a $^7Li^{16}O^1H$ target. The present results were obtained with a metallic ^7Li target and are considered to be more reliable than the older results. Figures 8–10 include both the new and old data. The discrepancies are not large enough to affect the main conclusions drawn from the present work.

Figures 11 and 12 show plots of the energy dependence of the $^7Li(p,\pi^-)^8B^*$ and $^7Li(p,\pi^+)^8Li^*$ reactions at constant t values of 0.525 and 0.425 GeV$^2/c^2$, respectively. A four momentum transfer squared of 0.525 GeV$^2/c^2$ is nearly the largest t value accessible at 489 MeV, and 0.425 GeV$^2/c^2$ is nearly the smallest t value accessible at 200 MeV. Thus these figures represent the largest range of t values for which a comparison can be made over this range of energies. Also shown in these figures, by the solid lines, is the energy dependence of the $pp\rightarrow d\pi^+$ reaction after transformation to the nuclear frame. The details of this transformation are discussed in Ref. 12. If

TABLE I. A list of differential cross sections and analyzing powers for the $^7Li(\vec{p},\pi^+)$ reaction leading to some final states of $^8Li^*$. The 250 and 354 MeV data whose c.m. angles are only quoted to two significant figures are from Ref. 9. All other data in these tables is new data from this work.

t	$\theta_{c.m.}$	$^8Li_{g.s.}$	$^8Li^*_{0.9808}$	$^8Li^*_{2.255}$
		$T_p=250$ MeV		
0.605	22	445(23) 0.25(0.05)	297(19) 0.24(0.06)	687(29) 0.17(0.04)
0.556	47	186(8) 0.09(0.04)	92.6(5.5) 0.35(0.06)	3919(11) −0.03(0.03)
0.516	61	107(6) −0.52(0.05)	39.6(3.6) 0.16(0.09)	199(8) −0.14(0.04)
0.474	74	68.9(6.4) −0.64(0.09)	14.3(3.2) 0.14(0.22)	119(11) −0.40(0.09)
		$T_p=280$ MeV		
0.552	38.8	710(20) 0.40(0.04)	426(16) 0.62(0.04)	952(23) 0.24(0.03)
0.502	54.2	216(7) 0.01(0.05)	94.9(4.6) 0.34(0.06)	327(8) −0.02(0.04)
0.453	67.1	64.7(1.8) −0.68(0.04)	17.6(0.9) 0.26(0.08)	116(2) −0.06(0.03)
0.402	79.1	50.0(1.6) −0.59(0.05)	9.9(0.7) −0.25(0.11)	67.4(1.9) −0.07(0.04)
0.351	90.6	29.2(0.9) −0.26(0.05)	10.1(0.5) −0.12(0.08)	45.6(1.1) 0.04(0.04)
0.301	102.0	21.5(0.7) 0.09(0.05)	6.8(0.4) −0.01(0.09)	38.1(1.0) 0.29(0.04)
0.251	113.9	8.6(0.4) 0.47(0.06)	4.9(0.3) 0.39(0.08)	18.9(0.5) 0.45(0.04)
		$T_p=354$ MeV		
0.551	21.3	1160(50) 0.23(0.06)	611(36) 0.24(0.07)	1400(50) 0.20(0.05)
0.549	22	1050(45) 0.29(0.04)	494(31) 0.32(0.06)	1310(51) 0.33(0.04)
0.514	33	554(23) 0.18(0.03)	248(12) 0.32(0.04)	851(23) 0.38(0.06)
0.467	44	196(6) −0.01(0.03)	98.9(4.4) 0.22(0.04)	315(8) 0.34(0.05)
0.410	55	79.6(5.1)	37.9(3.6)	149(7) 0.38(0.05)
0.396	57.4	101(5) 0.17(0.08)	29.7(2.8) 0.55(0.15)	154(6) 0.26(0.06)
0.374	61	59.4(4.0)	40.2(3.4)	107(6) 0.22(0.06)
0.352	64.7	57.4(3.8) 0.25(0.10)	20.8(2.2) 0.61(0.15)	90.1(4.7) 0.28(0.08)
0.283	75.5	33.7(1.7) 0.24(0.07)	7.7(0.8) 0.42(0.15)	34.2(1.7) 0.62(0.07)
0.220	84.8	24.6(1.4) 0.64(0.09)	9.6(0.9) 0.79(0.13)	38.6(1.8) 0.66(0.07)
		$T_p=489$ MeV		
0.485	20.7	245(13) 0.03(0.12)	115(9) 0.44(0.17)	329(15) 0.07(0.10)
0.451	27.6	181(9) 0.10(0.11)	57.2(5.1) 0.48(0.20)	219(10) 0.09(0.10)
0.402	35.6	60.1(3.4) −0.38(0.10)	20.0(1.9) 0.13(0.19)	103(4) −0.04(0.08)
0.352	42.3	31.1(1.7) −0.29(0.11)	8.4(0.9) 0.15(0.22)	55.9(2.3) −0.38(0.08)
0.302	48.2	25.4(1.2) −0.13(0.10)	3.7(0.5) 0.28(0.24)	27.0(1.3) −0.18(0.09)
0.252	53.6	13.3(0.8) 0.31(0.12)	3.2(0.4) −0.20(0.25)	22.1(1.1) 0.04(0.10)

TABLE II. A list of differential cross sections and analyzing powers for the ^{7}Li($\vec{p},\pi^-$) reaction leading to some final states of ^{8}B*. A systematic uncertainty of ±7%, and a relative point-by-point uncertainty of ±12% are quoted for this experiment.

t	$\theta_{c.m.}$	$^8B_{g.s.}$	$^8B^*_{0.78}$	$^8B^*_{2.32}$
		T_p=280 MeV		
0.554	38.8	9.1(0.8) −0.31(0.13)	6.3(0.7) 0.31(0.14)	7.5(0.7) −0.29(0.14)
0.505	54.2	9.1(0.5) −0.19(0.10)	5.2(0.4) −0.17(0.12)	5.8(0.4) −0.34(0.12)
0.455	67.2	6.1(0.3) −0.01(0.08)	2.2(0.2) 0.35(0.13)	3.5(0.3) −0.07(0.11)
0.404	79.3	4.1(0.3) 0.08(0.09)	1.4(0.1) 0.37(0.15)	2.6(0.2) −0.02(0.11)
		T_p=354 MeV		
0.553	21.3	18.2(1.3) −0.56(0.10)	20.0(1.3) 0.20(0.10)	33.0(1.7) −0.54(0.08)
0.503	36.3	11.1(0.6) −0.24(0.08)	7.6(0.5) −0.04(0.10)	8.3(0.5) −0.52(0.09)
0.454	47.2	6.6(0.4) −0.33(0.10)	3.4(0.3) 0.10(0.14)	5.1(0.4) −0.63(0.11)
0.399	57.4	5.1(0.3) −0.29(0.09)	2.4(0.2) −0.14(0.13)	3.4(0.2) −0.36(0.11)
		T_p=489 MeV		
0.486	20.7	2.9(0.4) −0.14(0.35)	0.6(0.2) −1.0(0.66)	3.7(0.5) −0.76(0.30)
0.453	27.6	2.5(0.3) −0.40(0.22)	1.4(0.2) 0.02(0.29)	3.6(0.3) −0.22(0.18)
0.403	35.6	1.8(0.2) −0.07(0.21)	0.9(0.1) −0.15(0.30)	2.5(0.2) 0.20(0.17)

the (p,π^+) reaction is dominated by a quasifree $NN\rightarrow N\Delta\rightarrow NN\pi^+$ process, one would expect the ^{7}Li(p,π^+) reactions to have an energy dependence similar to that of the $pp\rightarrow d\pi^+$ reaction.

The (p,π^-) data in Fig. 11 exhibit an energy dependence that is very similar to that of the (p,π^+) data. For all three final states and both reactions, the differential cross section rises with energy up to the Δ_{1232} invariant mass, and then falls. The fall in differential cross section above the Δ_{1232} invariant mass is slight for the (p,π^+) reactions, but is very pronounced for the (p,π^-) reactions.

The energy dependences shown in Fig. 12 are similar to those shown in Fig. 11 except, for both (p,π^+) and (p,π^-), the solid triangles representing the 200 MeV data are very high in relation to the other points at this t value (see also Figs. 5–10), and the falloff above the Δ_{1232} mass is much less pronounced. The sudden drop in differential cross section at energies above the Δ_{1232} invariant mass in the (p,π^-) reaction may be a signature of the Δ_{1232}, but studies of the energy dependence of the elementary $pn\rightarrow pp\pi^-$ reaction are needed to confirm this. The double-differential cross section of the $pp\rightarrow pn\pi^+$ reaction, in which the Δ_{1232} is known to play a dominant role, does not drop so sharply with energy because of the contributions of additional partial waves. Thus the observed energy dependence of the (p,π^-) differential cross section above the Δ_{1232} invariant mass may require some other explanation.

The energy dependence of the ^{7}Li$(p,\pi^-)^8$B* differential cross section is shown in Figs. 11 and 12. It is similar to the energy dependence of the ^{13}C(p,π^-)X reac-

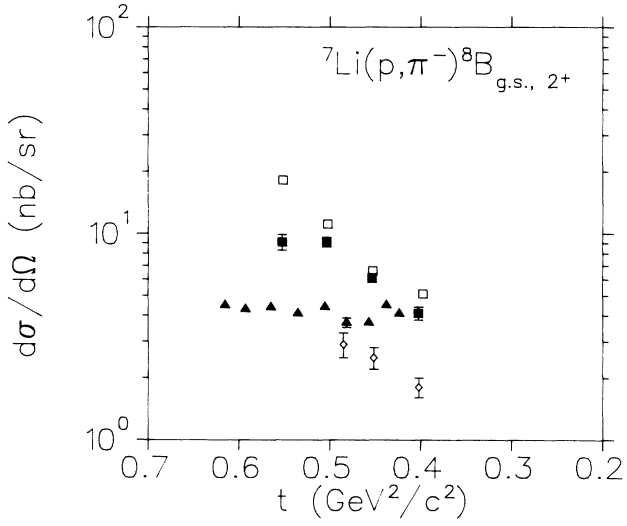

FIG. 5. Plot of differential cross section vs the square of the four momentum transfer for the ^{7}Li$(p,\pi^-)^8$B$_{g.s.}$ reaction. The plotting symbols indicate the source of data as follows: ▲, 200 MeV, Ref. 14; ■, 280 MeV, this work; □, 354 MeV, this work; ◇, 489 MeV, this work. The error bars reflect statistical uncertainties only.

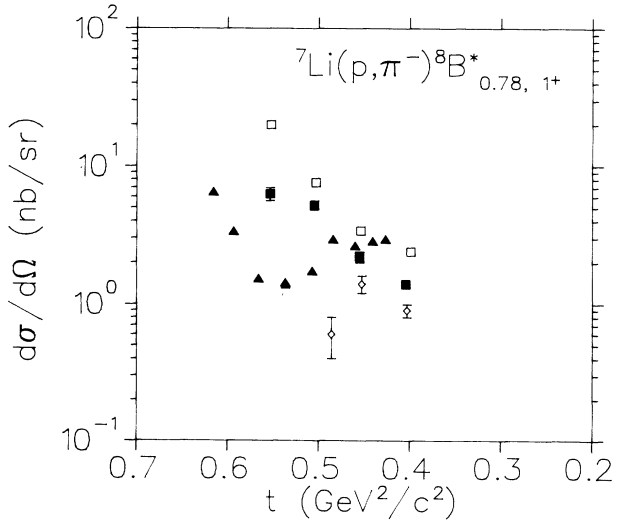

FIG. 6. Plot of differential cross section vs the square of the four momentum transfer for the ^{7}Li$(p,\pi^-)^8$B$^*_{0.78}$ reaction. The plotting symbols indicate the source of data as in Fig. 5.

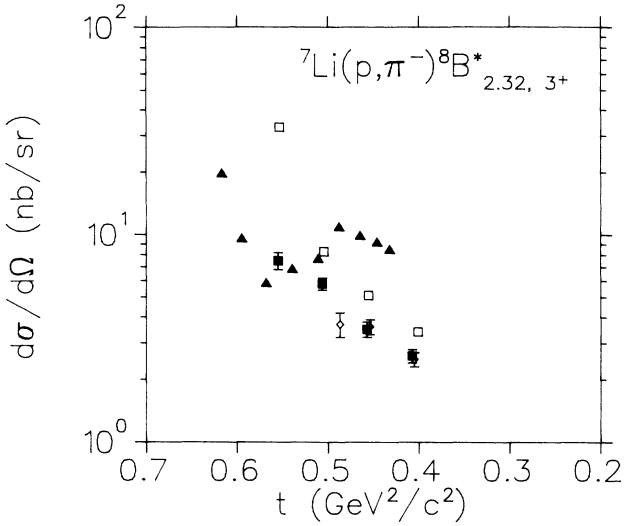

FIG. 7. Plot of differential cross section vs the square of the four momentum transfer for the $^7Li(p,\pi^-)^8B^*_{2.32}$ reaction. The plotting symbols indicate the source of data as in Fig. 5.

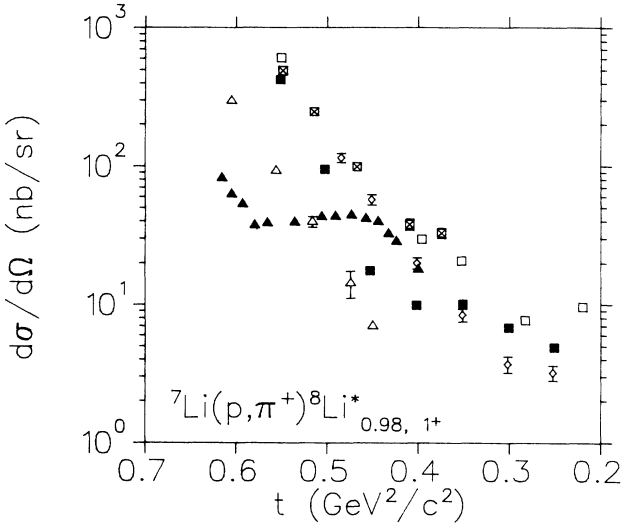

FIG. 9. Plot of differential cross section vs the square of the four momentum transfer for the $^7Li(p,\pi^+)^8Li^*_{0.98}$ reaction. The plotting symbols indicate the source of data as in Fig. 8.

tion to the continuum at $t=0.50$ GeV$^2/c^2$ (Ref. 12) and to that of the $^{18}O(p,\pi^-)^{19}Ne^*_{4.6}$ reaction at $q=608$ MeV/c.[13] However, the $^{13}C(p,\pi^-)$ reaction to discrete states of ^{14}O at $t=0.50$ GeV$^2/c^2$ exhibits an entirely different energy dependence (see Ref. 11).

Figure 13 shows the double-differential cross section of the $^7Li(p,\pi^-)X$ reaction for a 1 MeV wide bin of the continuum centered about an equivalent excitation energy of 15 MeV. As can be seen, the $^7Li(p,\pi^-)X$ continuum double-differential cross section is largest at 354 MeV for all t values. In the region of $t=0.50$ GeV$^2/c^2$, the double-differential cross section falls more rapidly between 354 and 489 MeV than at smaller t values. Thus Fig. 13 shows that the energy dependence of the $^7Li(p,\pi^-)X$ continuum reaction is similar to that of the $^7Li(p,\pi^-)^8B^*$ reaction to discrete final states.

A. Discussion

The present results, together with those in Refs. 11 and 12, show that all (p,π^+) reactions tend to have a "universal" energy dependence similar to that of the $pp\rightarrow d\pi^+$ reaction (after kinematic transformation), but that the energy dependence of the (p,π^-) reaction is sensitive to the nuclear transitions involved.

The (p,π^+) reaction in the Δ_{1232} region is known to be dominated by the underlying σ_{10} two-nucleon process

$$pp(^1D_2)\rightarrow\Delta N(^5S_2)\rightarrow pn(^3S_1)+P\text{-wave }\pi^+\ , \quad (1)$$

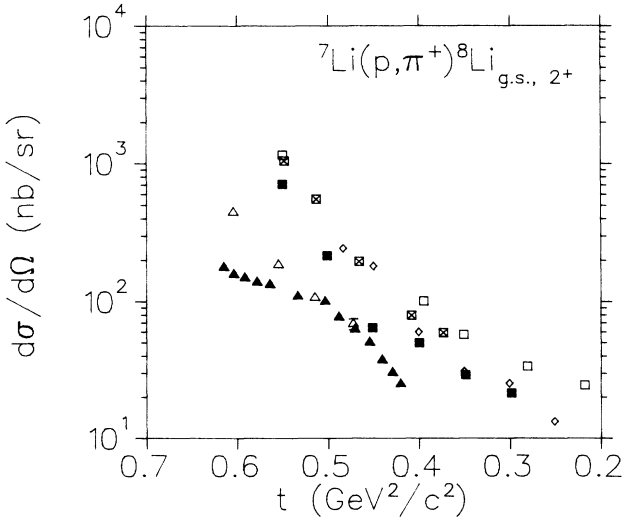

FIG. 8. Plot of differential cross section vs the square of the four momentum transfer for the $^7Li(p,\pi^+)^8Li^*_{g.s.}$ reaction. The plotting symbols indicate the source of data as in Fig. 5 except △, 250 MeV, Ref. 9; ⊠ 354 MeV, Ref. 9.

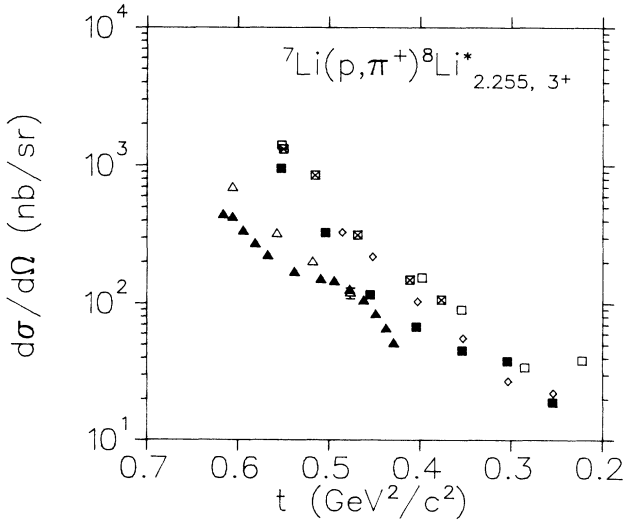

FIG. 10. Plot of differential cross section vs the square of the four momentum transfer for the $^7Li(p,\pi^+)^8Li^*_{2.255}$ reaction. The plotting symbols indicate the source of data as in Fig. 8.

where σ_{10} refers to the cross section for the case in which the two initial nucleons are in a $T=1$ state and the two final nucleons are in a $T=0$ state. For π^- production, the allowed Δ_{1232} channels in the underlying two-nucleon process are

$$pn(^3P_0)\rightarrow\Delta N(^3P_0)\rightarrow pp(^1S_0)+S-\text{wave }\pi^- \quad (2)$$

and

$$pn(^1D_2)\rightarrow\Delta N(^5S_2)\rightarrow pp(^3P_2)+S-\text{wave }\pi^- \quad (3)$$

involving P waves for either the intermediate ΔN or final NN state, as well as other channels involving still higher partial waves. These σ_{11} resonant amplitudes are much smaller than the σ_{10} amplitude that dominates the $pp\rightarrow pn\pi^+$ reaction[19,20] and may be partially masked in the (p,π^-) reaction by nonresonant amplitudes. Consequently, the energy dependence of the (p,π^-) reaction can be expected to be sensitive to the interference of several small amplitudes, whose relative importance can be influenced by nuclear structure.

The similarity between the energy dependences of the ^{7}Li(p,π^-) and ^{7}Li(p,π^+) differential cross sections shown here contrasts with the dissimilarities observed[11]

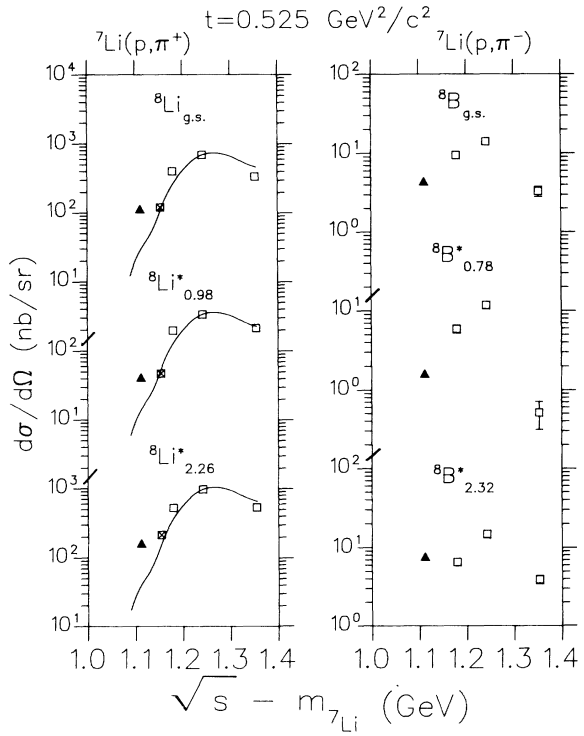

FIG. 11. Plot of differential cross section vs the excitation energy available for one nucleon $\sqrt{s}-m_{^7\mathrm{Li}}$ at a constant square of the four momentum transfer of 0.525 GeV$^2/c^2$ for both the ^{7}Li$(p,\pi^-)^8$B* and ^{7}Li$(p,\pi^+)^8$Li* reactions. The Δ_{1232} invariant mass occurs at an x axis value of 1.232 GeV. The plotting symbols indicate the source of the data as follows: ▲, Ref. 14, 200 MeV; ⊠, Ref. 9, 250 MeV; □, this work, 280, 354, 489 MeV. The solid curves are $pp\rightarrow d\pi^+$ differential cross sections transformed to the nuclear frame and normalized to the 354 MeV data points.

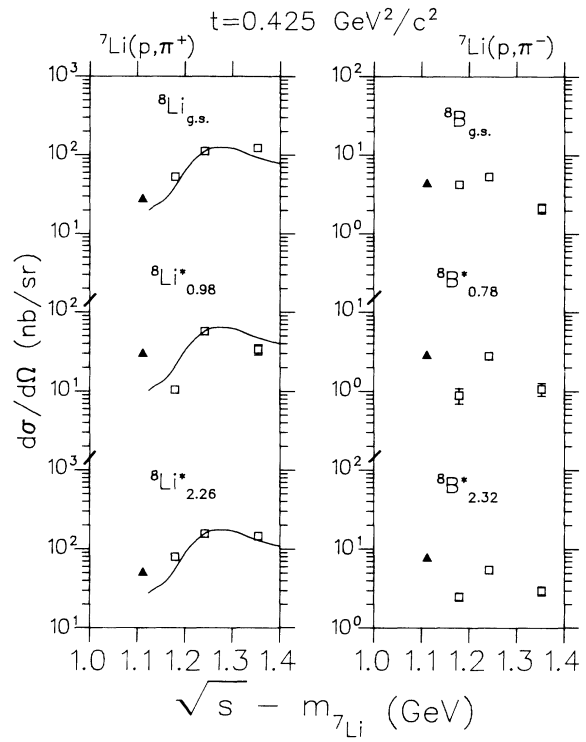

FIG. 12. Plot of differential cross section vs the excitation energy available for one nucleon $\sqrt{s}-m_{^7\mathrm{Li}}$ at a constant square of the four momentum transfer of 0.425 GeV$^2/c^2$ for both the ^{7}Li$(p,\pi^-)^8$B* and ^{7}Li$(p,\pi^+)^8$Li* reactions. The plotting symbols and the solid curve are as in Fig. 11.

for the ^{13}C(p,π^-) and ^{13}C(p,π^+) reactions and warrants an explanation. For the ^{13}C$(p,\pi^-)^{14}$O$_{g.s.}$ transition the two final protons are constrained by nuclear structure to be in a relative S state; hence the spin-isospin channel given by Eq. (3) above is forbidden. Equation (2) is allowed, but the apparent absence of any Δ contribution to

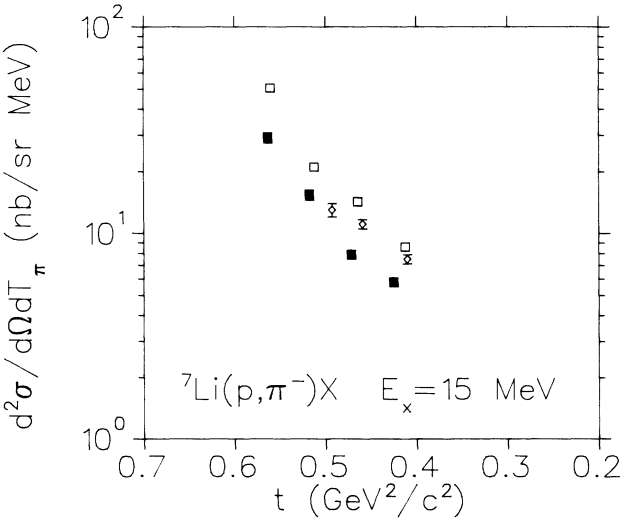

FIG. 13. Plot of the double-differential cross section of a 1 MeV wide portion of the ^{7}Li(p,π^-)X continuum taken at an equivalent excitation energy of 15 MeV. Plotting symbols are as in Fig. 5.

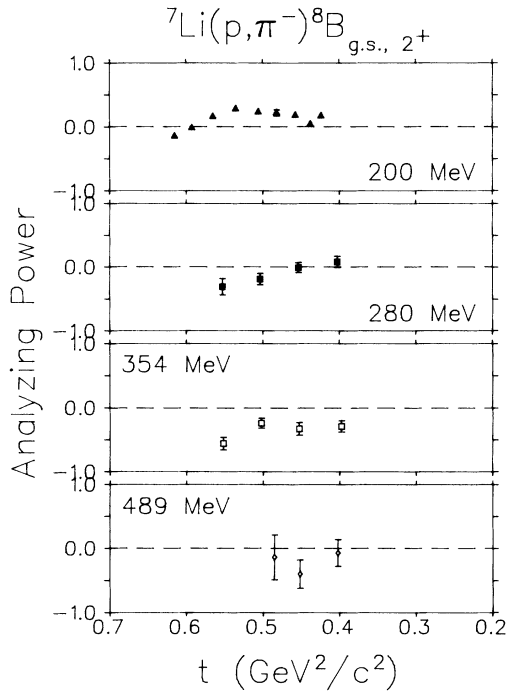

FIG. 14. Plot of analyzing power vs the square of the four momentum transfer for the $^7Li(\vec{p},\pi^-)^8B_{g.s.}$ reaction. The plotting symbols indicate the source of data as in Fig. 5. The error bars reflect statistical uncertainties only.

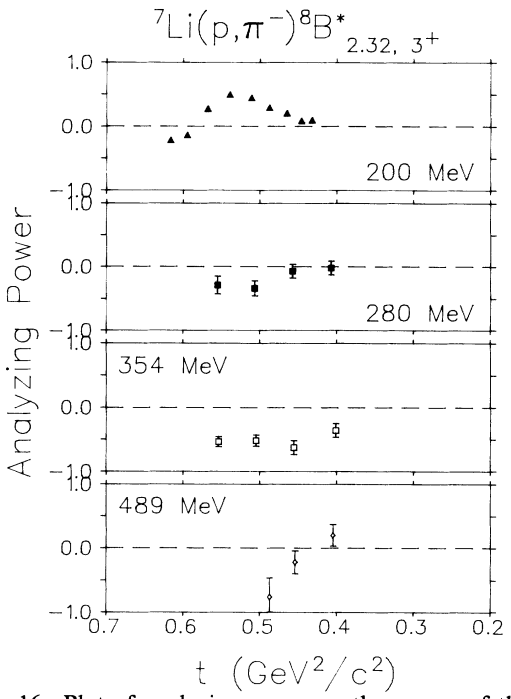

FIG. 16. Plot of analyzing power vs the square of the four momentum transfer for the $^7Li(\vec{p},\pi^-)^8B^*_{2.32}$ reaction. The plotting symbols indicate the source of data as in Fig. 5. The error bars reflect statistical uncertainties only.

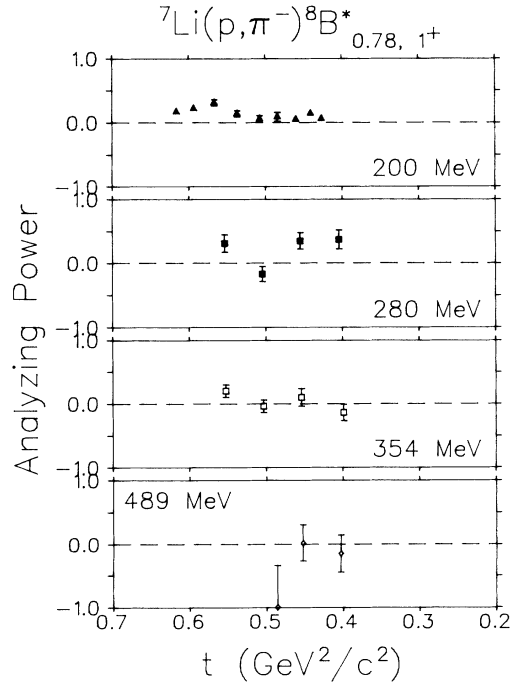

FIG. 15. Plot of analyzing power vs the square of the four momentum transfer for the $^7Li(\vec{p},\pi^-)^8B^*_{0.78}$ reaction. The plotting symbols indicate the source of data as in Fig. 5. The error bars reflect statistical uncertainties only.

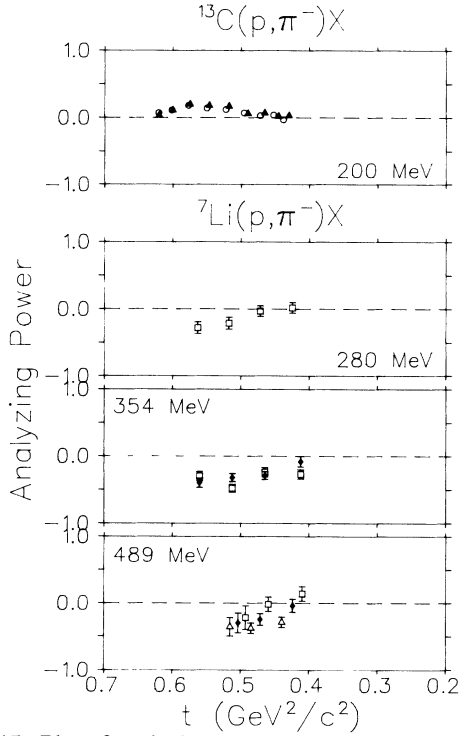

FIG. 17. Plot of analyzing power vs the square of the missing four momentum for a 1 MeV wide slice of the $^7Li(\vec{p},\pi^-)X$ continuum. The 200 MeV $^{13}C(\vec{p},\pi^-)X$ data is from Ref. 25, and has been used to indicate the approximate energy dependence of the analyzing power for the $(\vec{p},\pi^-)$ continuum. The 280, 354, and 489 MeV data is from this work. Plotting symbols indicate the equivalent excitation energies of the continuum slices as follows: ▲ 19 MeV; ○, 21 MeV; □, 15 MeV; ♦, 29 MeV; △, 45 MeV.

this transition suggests that this amplitude is very small, and that the $^{13}C(p,\pi^-)^{14}O_{g.s.}$ transition is dominated by nonresonant processes such as

$$pn(^3D_1, T=0) \rightarrow pp(^1S_0) + P\text{-wave } \pi^- \quad (4)$$

that cannot access an intermediate $\Delta N(T=1,2)$ state, as has been suggested by Vigdor *et al.*[21] (see also Ref. 11). For the $^{13}C(p,\pi^-)^{14}O^*_{6.27,6.59}$ transition, the final two protons are not constrained to be in a relative S state by nuclear structure, although it has been argued[22,23] that they may be so constrained by the short-range (high momentum transfer) nature of the interaction. Assuming that the energy dependence of the $^7Li(p,\pi^-)$ transitions are due to the influence of the Δ_{1232}, these arguments could account for the substantial differences observed between the energy dependences of the (p,π^-) reactions on ^7Li and ^{13}C. Detailed model calculations, and comparisons with forthcoming $pn \rightarrow pp\pi^-$ data,[24] are a necessary basis for an understanding of the dynamics of the (p,π^-) reaction.

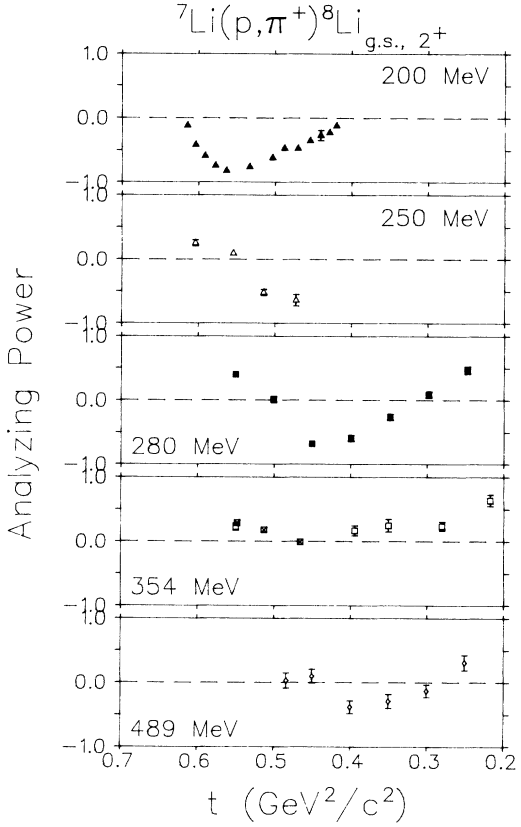

FIG. 18. Plot of analyzing power vs the square of the four momentum transfer for the $^7Li(\vec{p},\pi^+)^8Li_{g.s.}$ reaction. The plotting symbols indicate the source of data as in Fig. 5. 55° and 61° 354 MeV results from Ref. 9 have not been included in Figs. 18 and 19 because they disagreed substantially with the results of this work. These older analyzing powers are not considered as reliable as the new results because of the difficulty of subtracting the $^{16}O(\vec{p},\pi^+)X$ continuum from underneath a small low statistics peak. The error bars reflect statistical uncertainties only.

V. ANALYZING POWER SYSTEMATICS

Figures 14–16 show the analyzing powers of the $^7Li(\vec{p},\pi^-)^8B^*$ reactions. These are the first $(\vec{p},\pi^-)$ analyzing powers ever measured in this energy region. A systematic feature of the data is that the analyzing powers tend to become more negative as the energy increases. The analyzing powers for $^7Li(\vec{p},\pi^-)X$ to the continuum also exhibit this same general energy dependence, as shown in Fig. 17.

In contrast, the analyzing powers of the $(\vec{p},\pi^+)$ reactions shown in Figs. 18–20 become progressively more positive as the energy increases up to the Δ_{1232} invariant mass, and then become more negative again at higher energies. This type of energy dependence has been seen previously for other $(\vec{p},\pi^+)$ reactions,[10] and appears to be generally consistent with that of the $\vec{p}p \rightarrow d\pi^+$ process, which is shown by the solid lines in Fig. 20. This same energy dependence is exhibited by the $^7Li(\vec{p},\pi^+)X$ continuum reaction, as shown in Fig. 21.

Figures 14–21 show that the energy dependence of the $(\vec{p},\pi^-)$ analyzing powers is very similar to that of the $(\vec{p},\pi^+)$ analyzing powers, except for a difference in sign. This is shown more clearly in Fig. 22, which compares the analyzing powers of the $^7Li(\vec{p},\pi^-)^8B^*_{2.32}$ reaction, multiplied by -1, with the analyzing powers of the $^7Li(\vec{p},\pi^+)^8Li^*_{2.26}$ reaction. Since the two final nuclear

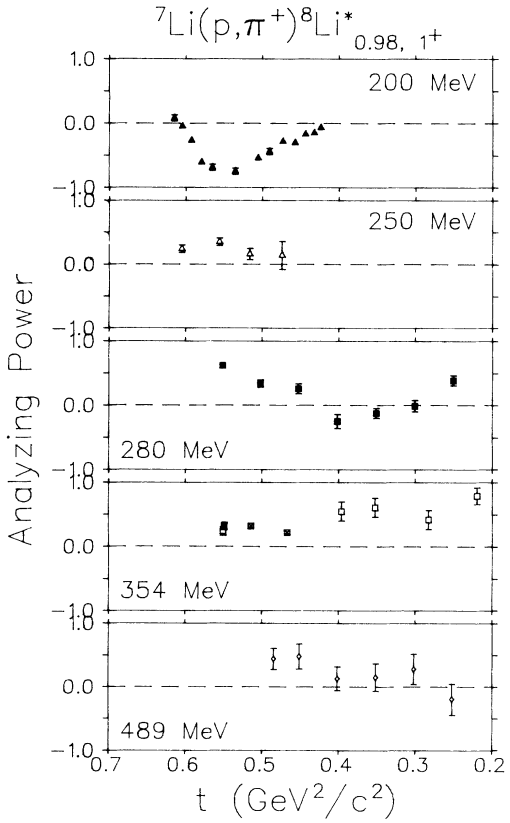

FIG. 19. Plot of analyzing power vs the square of the four momentum transfer for the $^7Li(\vec{p},\pi^+)^8Li^*_{0.98}$ reaction. The plotting symbols indicate the source of data as in Fig. 5. The error bars reflect statistical uncertainties only.

states are mirrors of each other, the difference in sign of the $(\vec{p},\pi^-)$ and $(\vec{p},\pi^+)$ analyzing powers must be a signature of the different scattering amplitudes involved in the two reactions. Hoistad *et al.*[27] have qualitatively explained the sign difference between the ^{9}Be($\vec{p},\pi^-$)^{10}C and ^{9}Be($\vec{p},\pi^+$)^{10}Be analyzing powers at 650 MeV in terms of the elastic and charge exchange $\pi N \rightarrow \pi N$ scattering amplitudes. Korkmaz[28] has suggested that the opposite signs observed for $(\vec{p},\pi^-)$ and $(\vec{p},\pi^+)$ analyzing powers may simply reflect the interchange of spin singlet and spin triplet NN states in the dominant amplitudes of the free $NN \rightarrow NN\pi$ processes $[(pp)^1D_2 \rightarrow (np)^3S_1\pi^+$ versus $(pn)^3D_1 \rightarrow (pp)^1S_0\pi^-]$.

It is tempting to assume that the analyzing power systematics observed here are general features of $(\vec{p},\pi^-)$ reactions, and that something may be learned about the yet unmeasured $\vec{p}n \rightarrow pp\pi^-$ analyzing powers from these data. This is suggested by the similarity of the ^{7}Li($\vec{p},\pi^+$) analyzing powers to those of the $\vec{p}p \rightarrow d\pi^+$ reaction after an appropriate kinematic transformation.[21] However, the correlation between $A(\vec{p},\pi^-)A+1$ and elementary $\vec{N}N \rightarrow NN\pi^-$ analyzing powers may be more complicated, due to the greater sensitivity of the (p,π^-) reaction to nuclear structure effects.

VI. SUMMARY AND CONCLUSIONS

Data for the ^{7}Li($\vec{p},\pi^-$)^{8}B* and ^{7}Li($\vec{p},\pi^+$)^{8}Li* reactions leading to discrete states and the continuum at $T_p = 280$, 354, and 489 MeV have been presented and compared with previously published 200 MeV results. The pion spectra show that low-lying discrete states are populated more weakly in relation to the continuum in the (p,π^-) reaction than in the (p,π^+) reaction.

The differential cross sections of the (p,π^-) reactions rise from $T_p = 200$ MeV to near the Δ_{1232} invariant mass at $T_p = 354$ MeV and then fall markedly at $T_p = 489$ MeV. This is in contrast to the energy dependence of the (p,π^+) differential cross sections, which also rise from 200 to 354 MeV but then either fall slowly, or not at all, at 489 MeV.

Comparisons with previously published ^{13}C$(p,\pi^\pm)$ data in this energy range show that the energy dependence of

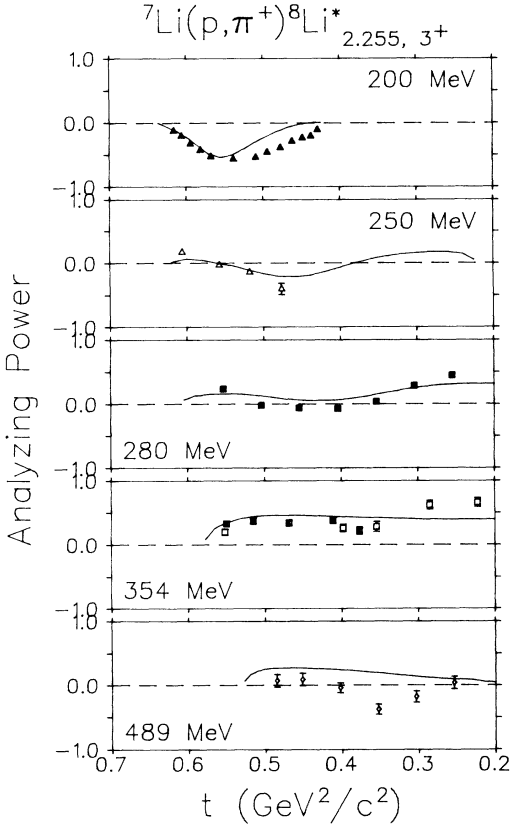

FIG. 20. Plot of analyzing power vs the square of the four momentum transfer for the ^{7}Li($\vec{p},\pi^+$)^{8}Li$^*_{2.25}$ reaction. The plotting symbols indicate the source of data as in Fig. 5. The error bars reflect statistical uncertainties only. The solid curves are $\vec{p}p \rightarrow d\pi^+$ analyzing powers after transformation to the nuclear frame. Although this transformation uses the $\vec{p}p \rightarrow d\pi^+$ data explicitly, it should yield a valid comparison with the analyzing power of $\vec{N}N \rightarrow NN\pi^+$ processes in general since the $\vec{p}p \rightarrow d\pi^+$ and $\vec{p}p \rightarrow pn\pi^+$ analyzing powers are very similar (Ref. 26).

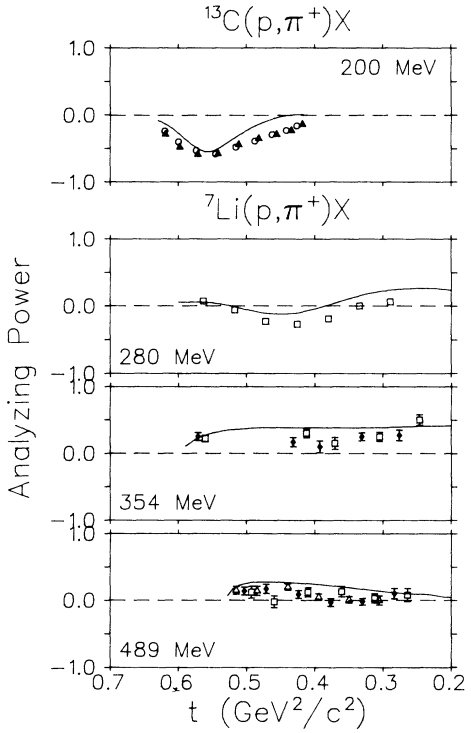

FIG. 21. Plot of analyzing power vs the square of the missing four momentum for the $(\vec{p},\pi^+)$ continuum. The 200 MeV ^{13}C$(\vec{p},\pi^+)$X data is from Ref. 25 to help show the approximate energy dependence of the $(\vec{p},\pi^+)$ continuum, and the remaining data points are from this work. The plotting symbols indicate the equivalent excitation energies as in Fig. 17 except ▲, 20 MeV; ○, 22 MeV. The solid curves are $\vec{p}p \rightarrow d\pi^+$ analyzing powers after transformation to the nuclear frame. There is no 354 MeV continuum data from Ref. 9 between $0.55 > t > 0.45$ GeV$^2/c^2$ because results from that work were obtained using a ^{7}Li^{16}O^{1}H target, and hence the ^{7}Li(p,π^+) continuum could not be separated from the ^{16}O(p,π^+) continuum.

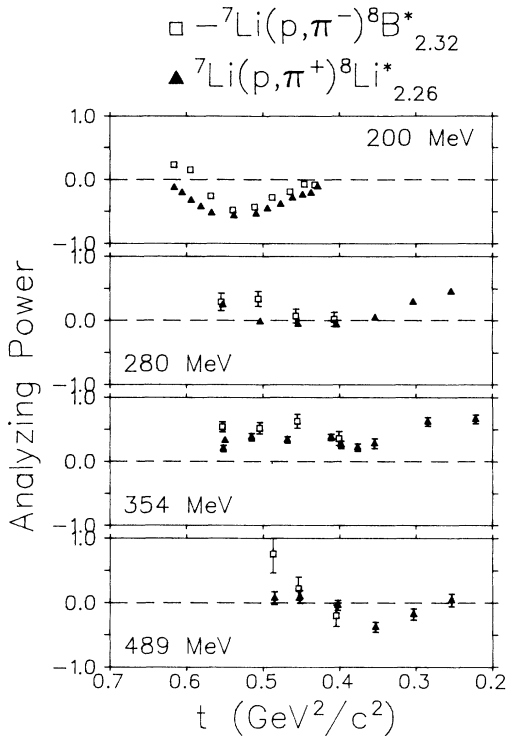

FIG. 22. Comparison of the $^7\mathrm{Li}(\vec{p},\pi^-)^8\mathrm{B}^*_{2.32}$ and $^7\mathrm{Li}(\vec{p},\pi^+)^8\mathrm{Li}^*_{2.26}$ analyzing powers after multiplying the $(\vec{p},\pi^-)$ analyzing powers by -1.

the (p,π^-) reaction is sensitive to the nuclear states involved, whereas the (p,π^+) reactions tend to have a "universal" energy dependence similar to that of the $pp\rightarrow d\pi^+$ reaction (after kinematic transformation). These results support the hypothesis that (p,π^+) reactions are dominated by a single underlying resonant $pp\rightarrow pn\pi^+$ spin-isospin channel involving an intermediate S-wave ΔN state and S-wave final nucleons, whereas several weak resonant and nonresonant amplitudes contribute to the (p,π^-) reaction, depending on the constraints imposed by nuclear structure.

The analyzing powers of the $(\vec{p},\pi^-)$ and $(\vec{p},\pi^+)$ reactions are very similar except that they have opposite signs.

Thus our understanding of the (p,π^-) reaction seems to have come full circle. Twelve years ago the (p,π^-) reaction was neglected because its featureless angular distributions did not arouse enough interest to merit the difficulty of measuring the very small (p,π^-) cross sections. These featureless angular distributions were taken as evidence of a multistep reaction mechanism.[29] Then, after the discovery of the (p,π^-) selectivity for stretched $2p$-$1h$ final states, it was suggested[30] that the (p,π^-) reaction might in fact be *easier* to understand than the (p,π^+) reaction, because the latter involves contributions from several different one- and two-nucleon processes and a summation over a variety of orbitals in the initial and final nuclear states. In contrast, in the (p,π^-) reaction the one-nucleon mechanism cannot contribute, and only one underlying two-nucleon process $(pn\rightarrow pp\pi^-)$ is involved. In some cases the orbitals of the active nucleons are tightly constrained by nuclear structure. The present work has shown, however, that the *reaction dynamics* of the (p,π^-) reaction may indeed be more difficult to understand than that of the (p,π^+) reaction because of the interference of several small resonant and nonresonant amplitudes that do not play a major role in the (p,π^+) reaction.

The gross features of the (p,π^-) and (p,π^+) reactions in the Δ_{1232} resonance region have now been mapped out by experiment. Detailed theoretical calculations, constrained by the data, are needed to sort out the dominant amplitudes in the (p,π^+) and (p,π^-) reactions.

ACKNOWLEDGMENTS

The authors would like to thank F. A. Duncan and E. G. Auld for their help during the experiment, C. A. Miller for assistance in using the MRS spectrometer, and D. Frekers for the updated data analysis program. This work has been supported by a grant from the Natural Sciences and Engineering Research Council of Canada (NSERC).

*Present address: Indiana University Cyclotron Facility, Bloomington, IN 47408.

†Permanent address: Department of Physics and Astronomy, Ohio University, Athens, OH 45701.

[1]D. F. Measday and G. A. Miller, Annu. Rev. Nucl. Part. Sci. **29**, 121 (1979).

[2]B. Hoistad, in *Advances in Nuclear Physics,* edited by J. W. Negele and E. Vogt (Plenum, New York, 1979), Vol. 11, p. 135.

[3]H. W. Fearing, in *Progress in Particle and Nuclear Physics,* edited by D. Wilkinson (Pergamon, New York, 1981), Vol. 7, p. 113.

[4]P. Couvert, in Proceedings of the Workshop on Studying Nuclei with Medium Energy Protons, edited by J. M. Greben, Edmonton, 1983, TRIUMF Proceedings Report TRI-83-3, 1983, p. 287.

[5]*Pion Production and Absorption in Nuclei-1981 (Indiana University Cyclotron Facility),* Proceedings of the Conference on Pion Production and Absorption in Nuclei, AIP Conf. Proc. No. 79, edited by R. D. Bent (AIP, New York, 1982).

[6]S. E. Vigdor *et al.*, Nucl. Phys. **A396**, 61c (1983).

[7]T. G. Throwe *et al.*, Phys. Rev. C **35**, 1083 (1987).

[8]G. M. Huber *et al.*, Phys. Rev. C **36**, 1058 (1987).

[9]G. M. Huber *et al.*, Phys. Rev. C **36**, 2683 (1987).

[10]G. M. Huber *et al.*, Phys. Rev. C **37**, 215 (1988).

[11]G. M. Huber *et al.*, Phys. Rev. C **37**, 1161 (1987).

[12]G. M. Huber *et al.*, Phys. Rev. C **37**, 2051 (1987).

[13]R. D. Bent, TRIUMF Annual Report of Scientific Activities, 1983, p. 35.

[14]Z. J. Cao *et al.*, Phys. Rev. C **35**, 825 (1987).

[15]G. M. Huber, Ph.D. thesis, University of Regina, 1988.

[16]C. A. Miller, in Proceedings of the Workshop on Studying

Nuclei with Medium Energy Protons, edited by J. M. Greben, Edmonton, 1983, TRIUMF Proceedings Report TRI-83-3, 1983, p. 339.
[17]G. L. Giles, Ph.D. thesis, University of British Columbia, 1985.
[18]D. Kurath, Phys. Rev. C **35**, 2247 (1987).
[19]W. O. Lock and D. F. Measday, *Intermediate Energy Nuclear Physics* (Methuen, London, 1970).
[20]B. J. VerWest and R. A. Arndt, Phys. Rev. C **25**, 1979 (1982).
[21]S. E. Vigdor, W. W. Jacobs, and E. Korkmaz, Phys. Rev. Lett. **58**, 840 (1987).
[22]H. Toki and K. I. Kubo, Phys. Rev. Lett. **54**, 1203 (1985).
[23]S. E. Vigdor, W. W. Jacobs, T. G. Throwe, and M. C. Green, Phys. Rev. Lett. **54**, 1204 (1985).
[24]N. E. Davison, private communication.
[25]E. J. Korkmaz *et al.*, Phys. Rev. Lett. **58**, 104 (1987).
[26]W. R. Falk *et al.*, Phys. Rev. C **32**, 1972 (1985).
[27]B. Hoistad *et al.*, Phys. Lett. **177B**, 299 (1986).
[28]E. J. Korkmaz, Ph.D. thesis, Indiana University, 1987.
[29]A. Reitan, in *Nuclear and Particle Physics at Intermediate Energies,* edited by J. B. Warren (Plenum, New York, 1976), p. 393.
[30]S. E. Vigdor *et al.*, Nucl. Phys. **A396**, 61c (1983).